

VI-I Photoionization and Photodissociation Dynamics Studied by Electron and Fluorescence Spectroscopy

Molecular photoionization is a major phenomenon in vacuum UV excitation and provides a large amount of information on fundamental electron-core interactions in molecules. Especially, neutral resonance states become of main interest, since they often dominate photoabsorption cross sections and lead to various vibronic states which are inaccessible in direct ionization. We have developed a versatile machine for photoelectron spectroscopy in order to elucidate dynamical aspects of superexcited states such as autoionization, resonance Auger decay, predissociation, vibronic couplings, and internal conversion. Two-dimensional photoelectron spectroscopy, allows us to investigate superexcited states in the valence excitation region of acetylene, nitric oxide, carbonyl sulfide, sulfur dioxide and so on. In this method, the photoelectron yield is measured as a function of both photon energy and electron kinetic energy (binding energy). The spectrum, usually represented as a contour plot, contains rich information on photoionization dynamics.

Photofragmentation into ionic and/or neutral species is also one of the most important phenomena in the vacuum UV excitation. In some cases, the fragments possess sufficient internal energy to de-excite radiatively by emitting UV or visible fluorescence. It is widely accepted that fluorescence spectroscopy is an important tool to determine the fragments and to clarify the mechanisms governing the dissociation processes of diatomic and polyatomic molecules. This year we have carried out fluorescence spectroscopy of OCS in the photon energy region of 15–30 eV.

VI-I-1 Formation and Autoionization of a Dipole-Forbidden Superexcited State of CS₂

HIKOSAKA, Yasumasa¹; MITSUKE, Koichiro
(¹Inst. Mater. Struct. Sci.)

[*J. Phys. Chem. A* in press]

Two-dimensional photoelectron spectroscopy has been performed in the photon energy region of 14.60–15.35 eV, in order to investigate forbidden superexcited states of CS₂. Figure 1 shows a two-dimensional photoelectron spectrum for the CS₂⁺($\tilde{B}^2\Sigma_u^+$) band and its vicinities. The electron yield is presented as a function of both photon energy $E_{h\nu}$ and ionization energy I_E by the plots with eight tones from light to dark on a linear scale. The curve in the right panel shows a constant ionic state spectrum, which is obtained by summing electron counts along the I_E axis at each $E_{h\nu}$. Five resonances of the Rydberg states converging to CS₂⁺($\tilde{C}^2\Sigma_g^+$) are observed at $E_{h\nu} = 14.69, 14.88, 14.95, 15.09,$ and 15.31 eV. The former two states are first assigned in this work. There exists remarkable vibrational excitation of one quantum of the anti-symmetric vibrational mode at $E_{h\nu} \sim 14.88$ eV. A similar excitation can be seen in the two-dimensional spectrum for the CS₂⁺($\tilde{X}^2\Pi_g$) band. This vibrational excitation is attributable to autoionization from a dipole-forbidden superexcited state which is formed through vibronic interaction with the $5p\sigma_u$ Rydberg state converging to CS₂⁺($\tilde{C}^2\Sigma_g^+$). The forbidden superexcited state is assigned as the $v = 1$ vibrational state in the v_3 mode of the $3d\sigma_g$ Rydberg member converging to CS₂⁺($\tilde{C}^2\Sigma_g^+$). Preference in the autoionization of the forbidden superexcited state was discussed.

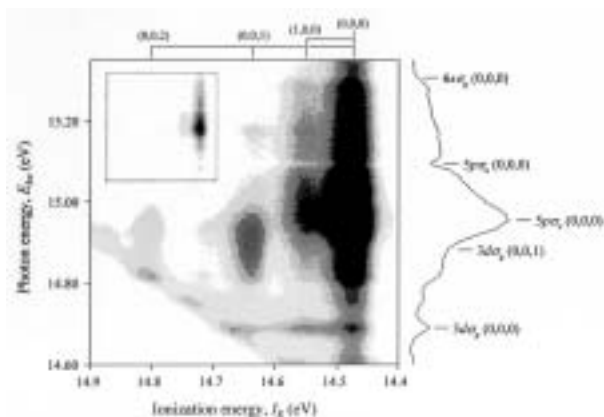


Figure 1. Two-dimensional photoelectron spectrum for the CS₂⁺($\tilde{B}^2\Sigma_u^+$) band and its vicinities measured in the photon energy range of 14.60–15.35 eV.

VI-I-2 UV and Visible Emission Spectra from Photodissociation of OCS Using Synchrotron Radiation at 15–30 eV

MITSUKE, Koichiro

Photofragmentation of OCS in the excitation photon energy range of 15–30 eV has been studied by dispersed fluorescence spectroscopy using monochromatized undulator radiation supplied from the UVSOR facility. Figure 1 shows dispersed fluorescence spectra of OCS encompassing the wavelength region of 360–530 nm at five photon energies between 19.85 and 29.8 eV. The following emission band systems have been identified: OCS⁺ [$A^2\Pi_{\Omega}(0,0,0) \rightarrow X^2\Pi_{\Omega}(0,0,v_3'')$], CO⁺ ($A^2\Pi_{\Omega} \rightarrow X^2\Sigma^+$), CS⁺ ($B^2\Sigma^+ \rightarrow A^2\Pi_{\Omega}$), and CO ($d^3\Delta \rightarrow a^3\Pi$). All the transitions except OCS⁺ [$A^2\Pi_{\Omega} \rightarrow X^2\Pi_{\Omega}$] are newly obtained from photodissociation of OCS in the vacuum UV region. The fluorescence excitation spectra for the OCS⁺ [$A^2\Pi_{\Omega}(0,0,0) \rightarrow X^2\Pi_{\Omega}(0,0,v_3'')$] and CS⁺ ($B^2\Sigma^+ \rightarrow A^2\Pi_{\Omega}$) transitions were measured in the photon energy range of 15.1–15.75 and 21.8–26 eV,

respectively. The emission spectra obtained at 20.85 and 22.9 eV exhibit atomic transitions of S [$nd^3D^o \rightarrow 4p^3P^e$ ($n = 6-9$)] which result from neutral dissociation of superexcited Rydberg states of OCS into S (nd^3D^o) + CO. Possible excited states of the counterpart CO were discussed on the basis of the difference in the n distribution between the two spectra.

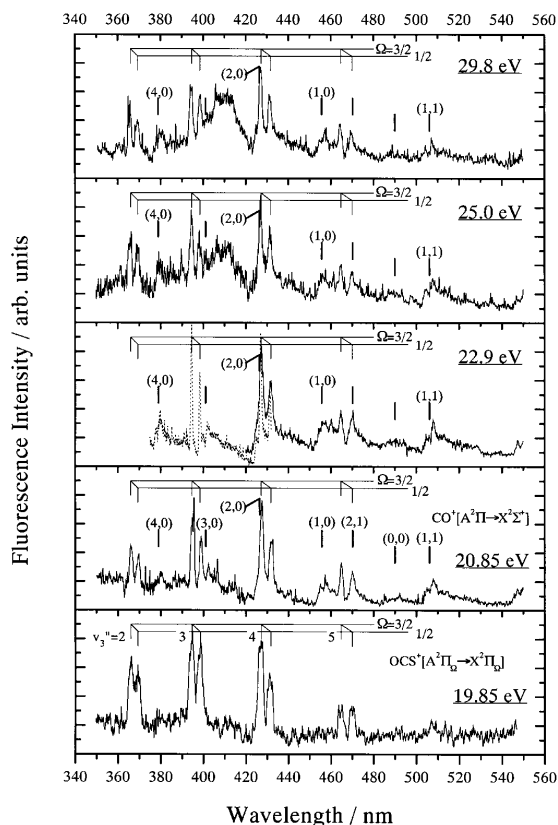


Figure 1. Dispersed fluorescence spectra of OCS encompassing the wavelength region of 360–530 nm at five photon energies between 19.85 and 29.8 eV. The thin vertical lines indicate the vibrational progression in the antisymmetric stretch v_3 mode of the OCS^+ [$A^2\Pi_{\Omega}(0,0,0) \rightarrow X^2\Pi_{\Omega}(0,0,v_3'')$] transition. The thick vertical lines indicate the band origins of the CO^+ ($A^2\Pi_{\Omega}, v' \rightarrow X^2\Sigma^+, v''$) emission-band system.

VI-J Development of a Laser-Synchrotron Radiation Combination Technique to Study Photoionization of Polarized Atoms

In conventional photoionization experiments, the most standard method has generally been taken to be measurement of energy and angular distributions of photoelectrons from randomly oriented (unpolarized) atoms or molecules. However, information obtained from these experiments is insufficient, since the initial state constituted of atoms and photons is not selected and the internal properties of final photoions and electrons are not analyzed. In this project, we have performed photoelectron spectroscopy of polarized atoms using linearly-polarized laser light, aiming at complete quantum-mechanical photoionization experiments. Initial excitation with a linearly polarized synchrotron radiation permits ensemble of atoms to be aligned along the electric vector of the light. From an angular distribution of photoelectrons from polarized atoms, we are able to gain insight into the magnitude and phase shift difference of transition dipole matrix elements of all final channels which are allowed by selection rules.

VI-J-1 Development of a Conical Energy Analyzer for Angle-Resolved Photoelectron Spectroscopy

IWASAKI, Kota¹; MITSUKE, Koichiro
(¹Shimadzu Co.)

[Surf. Rev. Lett. submitted]

A new angle-resolving electron energy analyzer composed of a conical electrostatic prism and position sensitive detector has been developed for gas-phase photoelectron spectroscopy. Performance tests have

been made in the energy and angular resolutions, transmission efficiency, and background level of the analyzer. Helium I photoelectron spectroscopy of Ar atoms was employed for the tests ($E_{\text{hv}} = 21.22$ eV). We fabricated a calibration cone electrode, on which a series of apertures of 0.5–2.0 mm in diameter are located as the test objects, and fitted this electrode in the analyzer to check the focussing efficiency by observing photoelectrons that pass through the apertures.

The 5.3 and 5.5 eV electrons produced by photoionization of Ar into $\text{Ar}^+(^2\text{P}_{3/2,1/2})$ were decelerated or accelerated and were made to pass through the analyzer. The photoelectron spectra were obtained by scanning the potential between the gas cell and inner cone electrode while the transmission energy is kept constant. The two peaks of the $\text{Ar}^+(^2\text{P}_{3/2,1/2})$ bands manifest symmetric Gaussian profiles, which reveals that the electric field acting upon the photoelectrons from the gas cell was not distorted. We have measured the energy resolution as a function of the transmission energy. The best energy resolution of 60 ± 1 meV (FWHM) has been achieved.

The angular resolution was evaluated from the extent of the image of the entrance apertures on the PSD detector. Figure 1 shows a typical electron image. Three spots correspond to the three entrance apertures of 1.5 and 2 mm in diameter. The angular resolution of 3° (FWHM) was estimated from the spot size for the aperture of 1.5 mm diameter. Taking into account the acceptance angle of 5.4° of the aperture from the sample

volume, we can conclude that the conical electrostatic prism has a convergence effect on the incident electrons in the azimuth direction. The diameter of the entrance aperture is the major determining factor of the angular resolution.

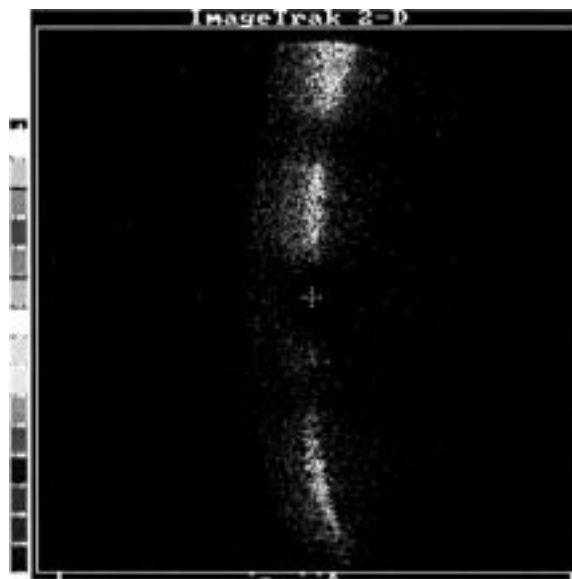


Figure 1. Photoelectron image on PSD. Three spots represent the image of three entrance holes bored on the inner cone electrode. The top spot was cut out by the edge of PSD.

VI-K Vacuum UV Spectroscopy Making Use of a Combination of Synchrotron Radiation and a Mode-Locked or Pulsed UV Laser

An ultraviolet laser system has been developed which synchronizes precisely with the synchrotron radiation (SR) from the storage ring of the UVSOR facility. A mode-locked Ti:sapphire laser is made to oscillate at the frequency of the ring in a multibunch operation mode. The delay timing between SR and laser pulses can be changed from 0 to 11 ns. The following combination studies have been performed: (1) two-photon ionization of helium atoms studied as the prototype of the time-resolved experiment, (2) laser induced fluorescence (LIF) excitation spectroscopy of $\text{N}_2^+(X^2\Sigma_g^+)$ ions produced by synchrotron radiation photoionization of N_2 or N_2O , and (3) LIF excitation spectroscopy of $\text{CN}(X^2\Sigma^+)$ radicals produced by synchrotron radiation photodissociation of CH_3CN .

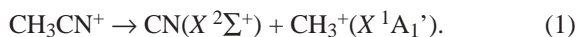
VI-K-1 Laser Induced Fluorescence Spectroscopy of $\text{CN}(X^2\Sigma^+)$ Radicals Produced by Vacuum UV Photoexcitation of CH_3CN with Synchrotron Radiation

MITSUKE, Koichiro; MIZUTANI, Masakazu

[*J. Electron Spectrosc. Relat. Phenom.* **119**, 155 (2001)]

Synchrotron radiation-pump and laser-probe spectroscopy is employed to observe CN radicals in the vibronically ground state produced from CH_3CN . The photon energy E_{SR} of synchrotron radiation is changed from 13.6 to 18.6 eV. The laser induced fluorescence

signal is measured as a function of E_{SR} with the laser wavelength fixed at the $\text{CN}(B^2\Sigma^+, v_B = 0 \leftarrow X^2\Sigma^+, v_X = 0)$ transition. The laser and monitored wavelengths were chosen at 388 and 420.8 nm, respectively. Figure 1 shows a plot of the LIF intensity, the difference between the fluorescence signal counts with and without the laser, as a function of E_{SR} . This plot represents the yield curve for the formation of $\text{CN}(X^2\Sigma^+, v_X = 0)$. The onset of 15.4 eV of the fluorescence signal indicates that the detected $\text{CN}(X^2\Sigma^+)$ radicals result from dissociative ionization of CH_3CN



The partial cross section for the formation of $\text{CN}(X^2\Sigma^+)$

is estimated to be 0.1–0.5 Mb and is in a reasonable agreement with that for the CH_3^+ formation.

In contrast to the photoionization efficiency curve of CH_3^+ , the LIF signal intensity in Figure 1 rapidly decreases beyond the peak at 15.6 eV and settle down to the background level at > 16 eV. The absence of the LIF signal above 16 eV is ascribed to a large kinetic energy release on the way of the dissociation of CH_3CN^+ . The quicker the $\text{CN}(X^2\Sigma^+)$ fragment escapes from the probe region, the lower its time-averaged number density becomes.

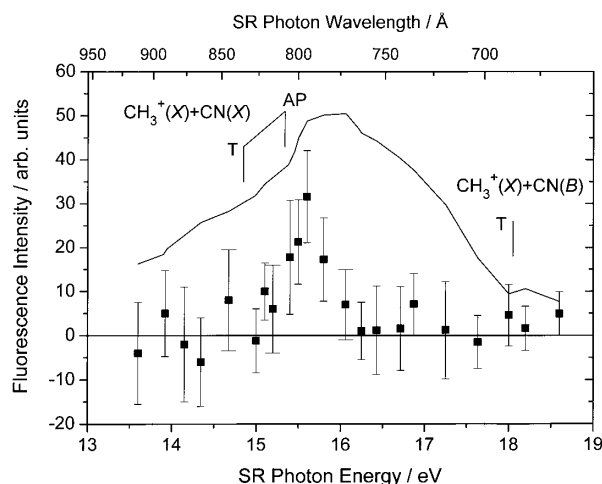


Figure 1. LIF signal intensity (\blacksquare) of the $\text{CN}(X^2\Sigma^+, v_X = 0)$ fragment produced from CH_3CN plotted against the SR photon energy. The solid curve represents the fluorescence excitation spectrum of CH_3CN for the $\text{CN}(B-X)$ emission. In both cases, the $(X^2\Sigma^+, v_X = 1) \leftarrow (B^2\Sigma^+, v_B = 0)$ transition was monitored.

VI-L Monochromator Newly Developed on the Beam Line BL2B2 in UVSOR

A grazing incidence monochromator has been constructed which supplies photons in the energy region from 20 to 200 eV. This monochromator will bridge the energy gap between the beam lines BL3A2 and BL8B1, thus providing for an accelerating demand for the high-resolution and high-flux photon beam from the research fields of photoexcitation of inner-valence electrons, L -shell electrons in the third-row atom, and $4d$ electron of the lanthanides.

VI-L-1 Performance of the 18 m-Spherical Grating Monochromator Newly Developed in the UVSOR Facility

ONO, Masaki; YOSHIDA, Hiroaki¹; HATTORI, Hideo²; MITSUKE, Koichiro
(¹Hiroshima Univ.; ²Nitto Tech. Inf. Cent. Co.)

[*Nucl. Instrum. Methods Phys. Res., Sect. A* **467-468**, 577 (2001)]

An 18 m-spherical grating monochromator with high resolution and high photon flux has been constructed at the bending magnet beamline BL2B2 of the UVSOR facility in the Institute for Molecular Science. The monochromator covers the energy range of 20–200 eV with three gratings. The resolving power ($E/\Delta E$) has been estimated by ion yield spectra of rare gas atoms (He, Ar and Kr) to be 2000–8000 under the conditions of a photon flux of 1×10^{10} photons s^{-1} and a ring current of 100 mA. A second-order light of 7% is contained at a photon energy of 45.6 eV.

VI-L-2 Anisotropy of Fragment Ions from SF_6 with Valence- and Sulfur L -Electron Excitation

ONO, Masaki; MIZUTANI, Masakazu; MITSUKE, Koichiro

Sulfurhexafluoride (SF_6) is one of the most well-known molecules that dissociate to multiple species of fragment ions after photoionization. In this research the asymmetry parameter β of the fragment ion has been measured in the energy region from the outer-valence to sulfur $2p$ electron excitation (23–200 eV).

The apparatus for the measurements of the anisotropy of fragment ions has been constructed at the end station of the beam line BL2B2 of UVSOR. The apparatus consists of two sets of an ion detector and three grids. The two ion detectors were mounted in the parallel and perpendicular direction to the electric vector of synchrotron radiation. The difference in the sensitivity between the two ion detectors are corrected by measuring the ion yield spectra of helium and argon atoms.

Figure 1 shows the fragment ion yield from SF_6 and β parameter. The spectrum covers a wide energy range from the outer-valence electron to sulfur $2p$ electron excitation. The three peaks at > 170 eV are assigned to the resonance excitations from $2t_{1u}$ (sulfur $2p$) to unoccupied valence orbitals ($6a_{1g}$, $2t_{2g}$ and $4e_g$). Several

features around 20–60 eV are found to resemble those in the absorption spectrum. The β parameter decreases with increasing photon energy. This trend can be explained qualitatively by the assumption that SF_5^+ ions has a much more anisotropic distribution than other fragments from SF_6 .

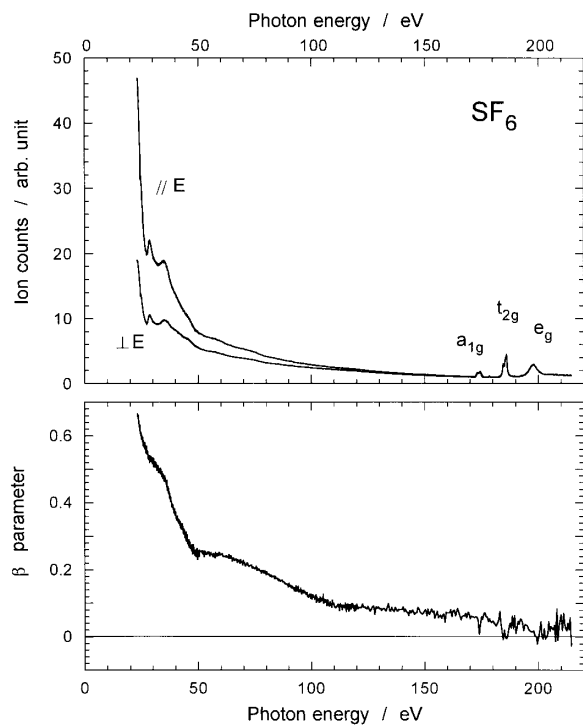


Figure 1. The fragment ion yield spectrum from SF_6 and asymmetry parameter β .